AIMS Materials Science, 10(1): 139–163.
DOI: 10.3934/matersci.2023008
Received: 30 September 2022
Revised: 25 December 2022
Accepted: 03 January 2023
Published: 18 January 2023

http://www.aimspress.com/journal/Materials

Research article

A versatile approach towards development of easy-to-clean transparent nanocoating systems with pronounced anti-static properties for various substrates

Nikolaos D. Papadopoulos[1,*], Pinelopi P. Falara[2] and Polyxeni Vourna[1,*]

[1] BFP Advanced Technologies, 11633, Athens, Attiki, Greece
[2] School of Chemical Engineering, National Technical University of Athens, 9 Ir. Polytech. St., Zografou, 15780, Greece

*** Correspondence:** Email: info@bfp-tech.com; Tel.: +00306932256264.

Abstract: Sol-gel is a widely applied method for the development of hydrophobic anti-soiling coatings. Most of them however suffer from serious drawbacks which restrict their generic applicability, especially on surfaces with limited number of hydroxyl groups. This study aims to propose a facile and straightforward strategy for the development of an "one-fits-all" anti-soiling coating with strong adhesion to a variety of hard, non-absorbent surfaces. The structure of the proposed composition is based on a two-component coating system consisting of an organopolysilazane primer and an alkoxysilane topcoat, based on a quaternarized ammonium silane. Morphology and microstructure were systematically studied, while hydrophobicity, adhesion, stability, abrasion and chemical resistance were determined on aluminum and PC substrates. The anti-soiling behavior of the proposed coating system was also evaluated. It was found that the polysilazane primer provided mechanical and chemical robustness regardless of substrate type, while the quaternarized silane offered pronounced easy-to-clean and anti-static attributes. The combination of such attributes within a single sol-gel coating system is highly beneficial for numerous applications.

Keywords: sol-gel; anti-soiling coatings; easy-to-clean; anti-static; organopolysilazane; quaternary ammonium silane

1. Introduction

In today's era, there is an increasing need to reduce effort and frequency of surface cleaning. The lifestyle of modern man combined with the increase in pollution sources have led to an abrupt increase of surface contaminants. At the same time, there is a growing skepticism regarding the use of common cleaners in everyday applications, since these often contain toxic ingredients. Hence, research efforts towards the development of effective substitutes of cleaning chemicals have been intensified. The most widespread method to date is to coat the surface with an anti-soiling film. Recent advances in nanotechnology have created expectations of definitely addressing the problems of pollution and surface contamination, through the development of invisible self-cleaning and easy-to-clean nano-coatings, either in do-it-yourself or industrially applied formats. In the last decade only, the impact that this technology had on the global market share of nano-coatings was tremendous; large companies as well as ambitious start-ups have released numerous products with highly promising anti-soiling attributes [1].

Transparent easy-to-clean coatings especially, have received considerable attention in scientific and industrial fields. There is a constantly increasing demand for the protection of surfaces which are commonly employed in various applications, devices and constructions of critical sectors, like energy, healthcare, building, transportation and optics. These are exposed to various pollutants, which penetrate their micropores. Among them, humidity, dust, lime scale and stains are the most common ones. In addition, variable conditions like ultraviolet radiation, high temperatures, acid rain and chemicals used for cleaning promote surface degradation, thus causing corrosion, color changes and mechanical wear. Scientific research has therefore focused on the fabrication of protective coatings for hard, non-absorbent surfaces, without changing their primary optical or haptic properties.

Anti-soiling coatings can be categorized into hydrophobic (mostly known as easy-to-clean) and hydrophilic (or self-cleaning) [2,3]. The latter exploits photocatalysis to decompose organic contamination. Since however most of the existing dirt is of inorganic nature primary interest has been given to the development of hydrophobic coatings. Throughout the years various low surface energy materials and techniques [4–16] have been used for the development of transparent water-repellent coatings. In terms of material cost and processing simplicity the use of alkoxysilanes and sol-gel perhaps present the most efficient combination of hydrophobic nanocoating fabrication [17–25].

However, the limited adhesion of alkoxysilane-based coatings on non-hydroxylated surfaces renders them improper for plastic substrates. To overcome this problem, special pretreatment, such as chemical and plasma etching or corona discharge is often necessary [3], which inevitably poses a serious practical limitation, especially in large scale implementations. Poor durability of sol-gel coatings is also an important matter of concern in the case of certain metals. Although physical properties, such as hardness, and morphological characteristics, such as smoothness, strongly affect the coating's mechanical stability, the primary factor for attaining robust structures is adhesion to the substrate.

A common practice for enhancing adhesion is increasing the substrate's wettability. Ghiotti et al. [26] enhanced wettability of AZ31 magnesium alloy substrates through surface texturing by means of Ultrasonic Vibration-Assisted Machining (UVAM) with cryogenic cooling. Substrates were dip coated by calcium phosphate (Ca-P) layers. The resulting thick coatings were crack-free. Surface texturing for increasing the wettability of the substrate was also employed by

Bertolini et al. [27]. It was found that the Ultrasonic Vibration Turning method improved surface wettability by creating a regular pattern, thus increasing deposition efficiency of a silane-based coating. However, inducement of surface texture led to a considerable increment of the coating's thickness.

Furthermore, a common way of increasing adhesion of sol-gel coatings on various substrates is the use of silane adhesion promoters. Syafiq et al. [28] fabricated transparent hybrid hydrophobic coatings with the aid of a PDMS binder, which promoted hydrophobicity and a 3-glycidoxypropyl trimethoxysilane (GLYMO), which in combination with 3-aminopropyltriethoxysilane (APTES) offered enhanced durability and adhesion on glass substrates. Increasing the amount of PDMS during the fabrication process enhanced hydrophobic properties. However, a rise in the concentration of GLYMO and APTES led to undesired effects, such as reduced transparency and limited adhesion. Finally, although self-cleaning properties were adequate, transparency maintenance in outdoor conditions was verified for a short exposure period of two months.

The use of both inorganic and organic polysilazane binders for the fabrication of self-cleaning coatings has also been reported. Chen et al. [29] prepared multilayer super-hydrophobic coatings on glass samples using an alkoxysilyl-substituted organopolysilazane as an 'anchor molecule'. The coating compositions consisted of alternate multilayers of the organopolysilazane binder and $(F\text{-}SiO_2)_n$ nanoparticles, where n represented the number of repeated bilayers, deposited via a layer-by-layer spray method. A supehydrophobic behavior was demonstrated when the multilayer coatings contained five bilayers. However, despite their excellent self-cleaning properties, they presented reduced transmittance due to increased absorption.

Finally, an additional method of producing mechanically robust structures is to incorporate a reactive polymeric binder into a silane solution. Polymeric binders offer flexibility and enhance the adhesion properties towards difficult-to-adhere substrates, such as painted and plastic surfaces. In addition, their reactivity allows the fabrication of durable and stable coatings giving rise to the development of functional properties, including enhanced corrosion-resistance, strong chemical and heat-resistance, as well as increased hardness and scratch-resistance [13,30]. Introducing hard metal-oxide or silica nanoparticles in the coating solution may further improve the coatings' mechanical stability. Suriano et al. [31] composed hydrophobic, sol-gel zirconia-based hybrid coatings with improved scratch resistance on polycarbonate substrates. A mixed oxide system consisting of silica and zirconium sols combined with a hydroxyl-functional fluoropolymer binder was employed. The binder was modified with the aid of an isocyanate-alkoxysilane, thus exhibiting good affinity between organic-inorganic components. The inorganic hybrid Zr-O-Si network had a glass transition temperature of 179 ℃, therefore the proposed coating seemed promising for outdoor exposure. Moreover, the pencil hardness of coated polycarbonate substrates was measured up to 4 grades higher, compared to the uncoated ones. It was suggested however, that adhesion to plastic substrates needed further improvement. It has been also reported [32] that priming aluminum plates and regular power windmill fan blades with polyurethane led to increased stability of the coating. The latter comprised PDMS and silica nanoparticles which promoted the development of a micro-structured surface, and thus the development of superhydrophobic attributes. An excellent anti-icing performance was also demonstrated.

In general, however, resin-based coatings have increased film-thicknesses which can reduce transmittivity and therefore, inhibit their applicability on high-end devices, such as electronics. Complex chemical processing, cumbersome application procedures and limited scalability may be

additional drawbacks.

It is evident that the development of anti-soiling coatings with pronounced resistance against abrasive wear and exposure to chemicals and UV radiation still remains problematic. In addition, maintaining the substrate's transmittivity after coating poses another technical challenge. Absorption losses from the coating itself can sometimes result in reduced transmittivity, thus restricting its utility, especially for optical applications. Last but not least, during the design of the coating system the potential hazards of certain sol-gel precursors, such as fluorosilanes [25], to human health and to the environment should not be neglected.

Within this work, a versatile approach towards development of eco-friendly, transparent and robust anti-soiling coatings in a facile way is presented. Emphasis is given on the microstructure and durability of the coating's structure, as well as on its ability to resist contamination and dust accumulation. The proposed coating is easy to apply and scale-up, therefore can be extensively employed in DIY applications, as well as by the coating industry. In addition, the scheme hereby proposed has universal applicability on non-porous substrates and is especially suitable for non-hydroxylated surfaces, such as plastics, where current sol-gel coatings fail to withstand excessive abrasion and prolonged exposure to UV and chemicals. Moreover, the coating becomes mechanically stable without complex surface pretreatment or texturing. The combination of the afore-mentioned attributes is, to our knowledge, unique in modern sol-gel based coating technology.

2. Materials and methods

The coating system was comprised by a polysilazane-based primer and an alkoxysilane-based topcoat. For the preparation of the primer, an organo-modified polysilazane precursor with reactive side groups, namely Si-H, Si-NH and Si-O-CH_2CH_3OH was used. For the synthesis of the anti-soiling coating, hydrolyzed tetraethoxysilane (TEOS) was aged in the presence of a quaternary ammonium silane (Si-QUAT). The latter acted both as a hydrophobizing agent and as an anti-static agent, while TEOS played the role of an anchor molecule. The coating was deposited on aluminum and polycarbonate (PC) substrates and subjected to various testing procedures focusing on those which are especially relevant to the coating industry.

2.1. Materials

A commercially available organopolysilazane, namely Durazane 1500 rapid cure (propyltriethoxysilyl-substituted polymethyl (hydro)/polydimethylsilazane) was supplied by Merck KGaA, Darmstadt, Germany. Tetraethoxysilane (TEOS, 98%) and a quaternary ammonium compound (3-trimethoxysilyl) propyl dimethyl octadecyl ammonium chloride, 72% in methanol), were supplied by Gelest Inc. Hydrochloric acid (fuming 37%), isopropyl alcohol (99.8%) and ethyl alcohol (99.5%) were all purchased from Sigma Aldrich. The chemicals were used as they were received. Deionized (DI) water was used as the solvent of coating solutions. Transparent polycarbonate thermoplastic sheets (10 cm × 10 cm, 3 mm thick) and bare, smooth aluminum 5005 plates (Q-panels, type AQ-46: 10 cm × 15cm, 0.8mm thick from Q-Lab) were used as substrates

2.2. Preparation and application of the coating system

Durazane 1500 rapid cure was diluted in butyl acetate at 2% v/v concentration. The solution was stirred moderately for 10 min, until the creation of a homogenous solution, which served as the primer. Then, synthesis of the top-coat solution followed. More specifically, 20 g of TEOS were dissolved into 180 g of a solvent mixture containing 10% w/w ethyl alcohol in water. The solution was acidified at pH = 2, by using 37% hydrochloric acid. The mixture was stirred vigorously for three hours until a homogenous liquid solution was formed. This solution was used as a concentrate batch. It was further diluted with water for the creation of three silica sols 200 mL each, containing 1%, 3% and 6% w/w of TEOS, respectively. To each of the above sols, a known amount of trimethoxysilyl propyl dimethyl octadecyl ammonium chloride (Si-QUAT) solution, 72% in methanol, was added under constant stirring. In all cases, the relative (TEOS:Si-QUAT) active content ratio in dry basis was kept constant at 4:1. The pH of each solution was then adjusted at pH = 4.5 by the addition of a NaOH aqueous solution concentrated at 1M. Moderate stirring continued for an additional time of two hours to ensure complete hydrolysis of Si-O-R ligands. The solutions were then transferred in closed vessels and aged for 24 h at ambient conditions to promote the development of quaternary ammonium-modified silica matrices. They were denoted as QAMS-1, QAMS-2, QAMS-3 (Table 1).

Three aluminum (Al) and three polycarbonate (PC) sheets were used as test substrates. Al sheets were degreased in an isopropyl alcohol solution (70% in water), while PC substrates were used as received. The OPSZ primer was applied manually with the aid of a clean microfiber pad. The topcoats were applied immediately onto the primer-coated substrates by a lens cleaning cloth. Then they were left to cure for 7 d at room temperature. For comparison reasons the topcoats were also applied on unprimed substrates.

Table 1. Chemical composition of silane top-coat solutions.

TopCoat	Ethanol (% w/w)	TEOS (% w/w)	Si-QUAT (%w/w)	Water (% w/w)
QAMS-1	0.90	0.99	0.35	97.76
QAMS-2	2.70	2.97	1.03	93.30
QAMS-3	5.29	5.88	2.06	86.77

2.3. Characterization

Coated samples were subjected to a series of tests and characterized by various techniques. Different coated samples were used for each test. More specifically, the static contact angles of coatings were measured at ambient temperature using an OCA 15EC video-based optical contact angle-measuring instrument (DataPhysics Instruments GmbH, Germany) equipped with SCA 20 software. Testing was performed with deionized water with an initial conductivity of less than 5 μS/cm. The contact angle was averaged over 6 measurements on the same surface. Advancing and receding contact angles were recorded, while 5 μL drop of the probe liquid was added to and withdrawn from the surface, respectively. During the growth/shrink of the water droplet the contour angle was measured. Each value was calculated by the average results of at least three measurements. Abrasion resistance of coatings was evaluated with the aid of a BYK 5063 Gardner-scrub wipe tester

(BYK-Gardner Gmbh, Germany), according to EN ISO 11998:2006 (standardized wet-scrub abrasion testing). A silicon carbide pad (Scotch-Brite Pad, No 7448, type S) was used for scouring the surface. Deionized water served as the liquid medium. The contact weight was 135 g. The scrub rate was 37 cycles/min and the stroke length was 25.4 cm. The water contact angle of abrasively worn surfaces was then measured in order to assess abrasion resistance of the coatings. Again, the contact angle was averaged over 6 measurements on the same surface. Adhesion was evaluated through cross-cut testing according to EN ISO 2409:2013. A single blade BYK 5125 cross-cut adhesion tester (BYK-Gardner Gmbh, Germany) with 1 mm spacing between cuts was used. The adhesive tape had an adhesion strength of 9 N/25 mm. The hydrolytic stability of coatings was determined by the loss on weight of coated samples after immersing them in deionized water at room temperature for 30 d. In order to evaluate the stability of coatings under UV irradiation, artificial weathering with fluorescent UV lamps, according to EN ISO 11507:2007, method A, took place inside a QUV/spray tester (Q-LAB Corporation, USA). The exposure condition was 4 h of UV radiation at 60 ℃, followed by 4 h of water condensation at 50 ℃. Fluorescent UVA-340 lamps were used as the light source, with the irradiance being 0.76 W/m^2 ·nm. The duration of the test was 1000 h. The water contact angle of the irradiated sample was recorded every 200 h in order to determine its resistance against UV. Chemical resistance was evaluated by modifying the standardized test method ASTM D1308-02(2013) which determines the effect of common chemicals and cleaners on clear organic finishes. The test was carried out by immersing the samples for 7 d in various liquid solutions. Then the reduction in WCA was measured in order to determine in a qualitative manner the coatings' chemical endurance. The surface topography of coatings was recorded by AFM. The microscope was equipped with a Nanoscope IIIA controller (Veeco Metrology, USA). Measurements were taken in ambient conditions by TESP cantilevers with nominal spring constants of 20–80 N/m (Bruker AXS). Images were recorded over areas of 1 × 1 μm. Different areas of each coating were visualized and the mean surface roughness was evaluated by the instrument's integrated software. SEM analysis was also implemented in order to study morphological characteristics and cohesion to the substrate of primed coated specimens. A Jeol JSM 6610LV Scanning Electron Microscope was used. Micrographs were taken with 3kV accelerating voltage, and a working distance of 5 mm. Imaging was carried out with secondary electrons. Both cross-section and plane view images were recorded. The coated specimens studied in cross-section were prepared as follows: First, they were cut on a microtome at slow speed to avoid delamination at the edges. Then, they were cold mounted in a polymer mold in such a way that their cross-section was exposed on the surface of the mold and were ground using up to 2000 SiC grit abrasive paper. The samples were then rinsed with distilled water and dried with compressed air. Finally, the anti-static behavior of coated specimens was evaluated through a series of soiling, with dust, test cycles, developed in-house. Samples were placed vertically on the sides of a cylindrical glass chamber containing at its bottom a graduated beaker with a stirring bar. The chamber was mounted on a magnetic stirrer hotplate. Sand dust with particle sizes of less than 150 μm was placed inside the beaker and airborne dust was created by the movement of the stirring bar at high speeds. At the top of the chamber a four-blade propeller located in the middle produced an air stream, which impinged the airborne particles on the coated substrates. In order to obtain reproducible soiling of coated samples the dust load was kept constant at 2 g/cm^2. Five soiling cycles were implemented, each one following a specific sequence: First, the substrate was immersed in distilled water for 5 min. Then, dust was applied. Subsequently, the substrates were dried for 24 h. The first and fifth cycle included one more step of washing with distilled water for 30 s. Dust

accumulation was indirectly evaluated by the drop in transmittivity of coated samples. Measurements were carried out in the wavelength range of 240–800 nm by a UV-Vis Hitachi 3010 spectrophotometer equipped with one $BaSO_4$ integrating sphere.

3. Results and discussion

The use of OPSZ facilitated the development of a strong crosslinked network between the primer and the topcoat. Organic polysilazanes possess alternating silicon and nitrogen atoms, thus leading to Si-N-Si structural frameworks. In comparison to common silanes and silicon compounds, they can be converted into organic/inorganic pre-ceramic materials. Because of their structure and their reactivity in the presence of moisture, they are compatible with either siloxane or silicon-based materials having a reactive functional group (i.e., a silanol group). Hence, they can be transformed into colloidal solutions after proper hydrolysis and polycondensation reactions and create hard, solid materials [33,34], even on non-hydroxylated surfaces.

It was found that increased concentrations of OPSZ (5% and up to 20%) led to higher film thicknesses and that endurance and anti-soiling performance in such cases were dictated by the primer's properties. Concentrations of OPSZ in the primer solution between 1 and 3% proved to be optimum, since these represented the best possible combination of satisfactory mechanical stability and adequate adhesion to non-hydroxylated surfaces. Therefore, in order to accurately assess the performance of the top coat itself the primer solution used had in all tests an OPSZ concentration of 2%. Inevitably, the primer's film thickness remained low, which seemed to give rise to a fast-curing process, activated by moisture. This process led to condensation of Si-H, Si-NH, and Si-O-CH_2CH_3OH groups into siloxane bonds (Figure S1 of Supplementary Information).

The primer became dry to the touch immediately after its application, thus allowing subsequent deposition of the topcoat. Reaction of the OPSZ with moisture generated groups which bound to the residual silanol groups of alkoxysilanes used in the topcoat. The two layers cured simultaneously thus behaving as a one-coating system. This process dramatically improved the coating's adhesion, stability and abrasion resistance, especially on PC substrates. At the same time, due to the low concentration of OPSZ, its impact on topcoat's features like hardness and surface energy was negligible.

It should be also noted, that by separately pre-hydrolyzing tetraethoxysilane and Si-QUAT (Figure S2 of Supplementary Information) the abrasion resistance of the coating system seemed to improve significantly.

Hydrolysis and subsequent condensation between tetraethoxysilane and trimethoxysilane molecules promoted a dense three-dimensional Si-O-Si network (Figure 1). Then the stability of this network improved further during co-curing with the underlying primer layer.

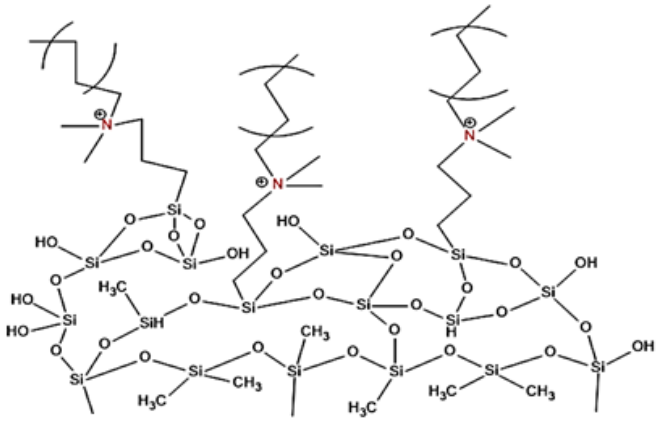

Figure 1. Illustration of the condensed top coat's structure.

Hydrolysis and condensation reactions were closely related to solution pH changes. Hydrolysis of ethoxy- and methoxy- substituted alkoxysilanes was facilitated at low pH values (≤3), while the condensation process was increased at pH values around 5. During the hydrolysis of TEOS and of quaternary ammonium silane at pH = 2, a fully hydrolyzed state of silanol groups occurred with minor interactions between the silica particles. The subsequent raise of the pH value at 4.5 assisted grafting of long Si-QUAT macromolecules to the silanol groups of tetraethoxysilane. As a result, a strong cohesive strength was developed between the hydrolyzed moieties and the entire condensed structure was able to graft onto the reactive groups of the polysilazane primer.

3.1. Measurement of static water contact angles

Hydrophobic and easy-to-clean properties were evaluated according to the values of static water contact angle (WCA) measured on aluminum and PC substrates, both with and without the primer. It was found that the WCA of uncoated aluminum substrates was in the order of 70 º ± 2 º. The highest hydrophobicity was displayed when the weight ratio (dry content) between TEOS and Si-QUAT was 2.97:1.03, respectively (Table 2). The three coating solutions were tested first on unprimed aluminum substrates to evaluate their surface energies regardless of the primer's impact. As it can be observed from Table 2, the most significant change in the measured values of WCA between unprimed and primed coated substrates was recorded for sample QAMS-1. The relatively low WCA value (87 º) without the primer indicated that the topcoat's amount of solids was probably insufficient, which might also affected adequate wetting of the substrate. In the case of QAMS-2 and QAMS-3 samples the measured differences in WCAs between primed and unprimed substrates were almost identical (±1 º).

Table 2. Results of the measured values of static WCAs of topcoats on aluminum substrates.

Sample	Weight Ratio (TEOS:Si-QUAT)	WCAs on coated Al without primer	WCAs on coated Al with primer
QAMS-1	0.99:0.35	87.0 º ± 2.2 º	93.0 º ± 1.0 º
QAMS-2	2.97:1.03	94.5 º ± 2.3 º	95.5 º ± 1.0 º
QAMS-3	5.88:1.06	93.0 º ± 2.3 º	93.8 º ± 1.0 º

The primer seemed to affect the attained hydrophobicity more significantly on PC substrates (Table 3). The measured WCAs of uncoated PC was in the order of 75 º ± 2 º. The low surface energy of PC rendered wetting from aqueous solutions problematic. Combined with the absence of free hydroxyl groups bonding and performance of the coating on unprimed PC substrates was rather poor, especially at low levels of topcoat's solids.

Table 3. Results of the measured WCAs of topcoats on PC substrates.

Sample	Weight ratio (TEOS:Si-QUAT)	WCAs on coated PC without primer	WCAs on coated PC with primer
QAMS-1	0.99:0.35	77.2 º ± 4.2 º	87.0 º ± 1.5 º
QAMS-2	2.97:1.03	88.0 º ± 3.5 º	95.0 º ± 1.5 º
QAMS-3	5.88:1.06	91.0 º ± 3.2 º	93.3 º ± 1.5 º

However, when the substrate had been treated with the OPSZ primer the measured WCA was significantly increased. Interestingly, it was noticed that after the deposition of QAMS-2 onto the primer, both aluminum and PC substrates demonstrated high values of WCAs, which were measured in both cases around 95 º. This finding implied independence of attained surface energy on the type of substrate, provided that the latter was primed. In addition, it seemed that a minimum amount of solids (around 4% w/w) in the topcoat solution was necessary in order a satisfactory hydrophobicity to be exhibited, regardless of substrate type. This was attributed to the role of TEOS which acted as an anchor molecule on which the quaternary ammonium silanes could graft. As concentration of TEOS increased it ultimately reached a point where a three-dimensional out-of-plane configuration was assumed, with long aliphatic chains to repel water in all directions. Due to the four hydrolysable groups of TEOS, the formation of a dense network was facilitated, which permitted the quaternarized silane to graft stronger and form a thicker film. In the absence of TEOS, stable anchoring of the quaternary ammonium silane on the OPSZ primer via its three hydrolysable groups would be difficult due to steric hindrance. In addition, the C-18 lipophilic chain of Si-QUAT (Figure S2) enhanced hydrophobicity of the coating and this effect got larger for higher amounts of TEOS which, in turn, promoted consistency and uniformity in the film thus formed.

With regards to dynamic contact angle measurements, the recorded advancing and receding water contact angles on Al and PC substrates are presented below (Tables 4 and 5).

Table 4. Advancing and receding WCAs of topcoats on Al substrates.

Sample	Advancing WCAs on coated Al without primer	Receding WCAs on coated Al without primer	Advancing WCAs on coated Al with primer	Receding WCAs on coated Al with primer
QAMS-1	87.5 º ± 2.2 º	65.1 º ± 2.1 º	94.0 º ± 2.3 º	74.7 º ± 2.1 º
QAMS-2	95.5 º ± 2.3 º	68.8 º ± 2.2 º	98.4 º ± 2.3 º	79.9 º ± 2.2 º
QAMS-3	93.2 º ± 2.3 º	59.5 º ± 2.1 º	94.4 º ± 2.3 º	69.4 º ± 2.1 º

Table 5. Advancing and receding WCAs of topcoats on PC substrates.

Sample	Advancing WCAs on coated PC without primer	Receding WCAs on coated PC without primer	Advancing WCAs on coated PC with primer	Receding WCAs on coated PC with primer
QAMS-1	80.2 º ± 2.2 º	54.9 º ± 2.1 º	92.4 º ± 2.2 º	66.9 º ± 2.1 º
QAMS-2	90.5 º ± 2.2 º	67.6 º ± 2.2 º	99.8 º ± 2.3 º	84.7 º ± 2.3 º
QAMS-3	92.7 º ± 2.2 º	72.2 º ± 2.2 º	95.6 º ± 2.2 º	75.8 º ± 2.3 º

The relatively high hysteresis values of all unprimed coated samples were attributed to surfaces roughness and chemical heterogeneity. Hysteresis of primed coated samples, especially of PC samples, was found to be much lower, which implied that the adhesion between water droplets was reduced. This behavior was attributed to the dominating role of the primer in improving topography and covering surface irregularities. The lubricating features of the topcoat might have further improved mobility of water droplets.

3.2. Abrasion resistance test

The above coated samples were subjected to 200 cycles of wet scrub abrasion to evaluate their mechanical strength and coherence. Both unprimed and primed aluminum and polycarbonate samples were tested. The reduction in WCA values after abrasion were used to interpret results. It was found that the OPSZ primer significantly contributed to the mechanical stability of the coatings and to retention of their anti-soiling attributes (Table 6). This finding was more apparent on PC substrates where hydrophobicity of unprimed coated samples seemed to completely vanish after abrasion, implying poor adherence to the substrate, due to lack of available hydroxyl groups. Furthermore, changes in the topcoat's weight of TEOS (and of total solids) also affected the coatings' hydrophobicity. It was noticeable that when the amount of TEOS increased from about 3% to about 6%, the coating's abrasion resistance dropped off. This could be explained by the excess of alkoxysilanes which could not condense on the primer. In addition, a strong correlation between hydrophobicity and abrasion resistance was depicted. It seemed that coatings with higher WCAs, exhibited better abrasion resistance, thus highlighting the role of the low-surface energy OPSZ primer in the strengthening of the coating's matrix.

Table 6. Measured static WCAs after abrasion.

Sample	WCAs after 200 abrasion cycles on coated Al without primer	WCAs after 200 abrasion cycles on coated Al with primer	WCAs after 200 abrasion cycles on coated PC without primer	WCAs after 200 abrasion cycles on coated PC with primer
QAMS-1	80.8 ° ± 2.2 °	89.1 º ± 1.7 º	74.0 º ± 1.0 º	83.7 º ± 2.0 º
QAMS-2	90.5 ° ± 2.2 °	93.2 º ± 1.7 º	75.4 º ± 0.9 º	91.9 º ± 1.5 º
QAMS-3	87.7 ° ± 2.2 °	90.2 º ± 1.7 º	75.1 º ± 0.5 º	86.4 º ± 2.1 º

Apparently, abrasion resistance of coatings on aluminum substrates was enhanced due to the high density of surface hydroxyl groups on its surface, which allowed strong adhesion of both the OPSZ primer and the top coat, through covalent bonding. The same observation also stands even for the sample with the lowest weight of total solids; even if the initial WCA of the coating was relatively low (87 º) its strong affinity with the substrate protected it from being completely destroyed after abrasion. Moreover, when primed, the WCA of the same sample (89.1 º) remained after abrasion close to the easy-to-clean threshold of 90 º, which indicated the necessity of the primer in attaining long-term functionality even on hydroxylated surfaces (Figure 2). This necessity became essential in the case of non-hydroxylated surfaces, such as PC (Figure 3).

The influence of abrasion on hydrophobicity of PC substrates was studied in more detail, i.e., the afore-mentioned abrasion test was performed in a stepwise manner, which corresponded to four abrasion intervals of 50 cycles each, namely 50, 100, 150 and 200 abrasion cycles. Among the three samples, QAMS-2 was the only one evaluated since it clearly demonstrated the best performance, regardless if the substrate was primed or not. Different PC substrates were used for each one of the abrasion intervals. The contact angle was averaged over 6 measurements on the same surface and the mean values are illustrated in Figure 4.

It was found that unprimed coatings on PC substrates had a rather limited abrasion resistance even after just 100 cycles. Priming the surface before coating significantly improved abrasion resistance. Interestingly, it was found that abrasion resistance of primed coated Al substrate was almost constant within the range tested. This was attributed to the primer's ability of stabilizing the entire coating structure and increasing its coherency.

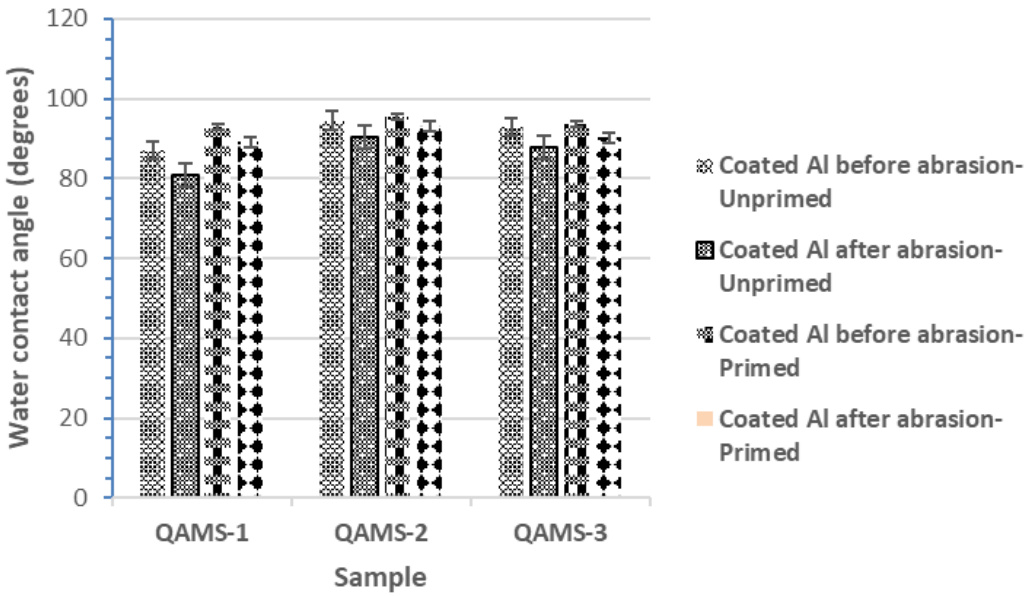

Figure 2. Changes in hydrophobicity of coatings on aluminum substrates before and after abrasion.

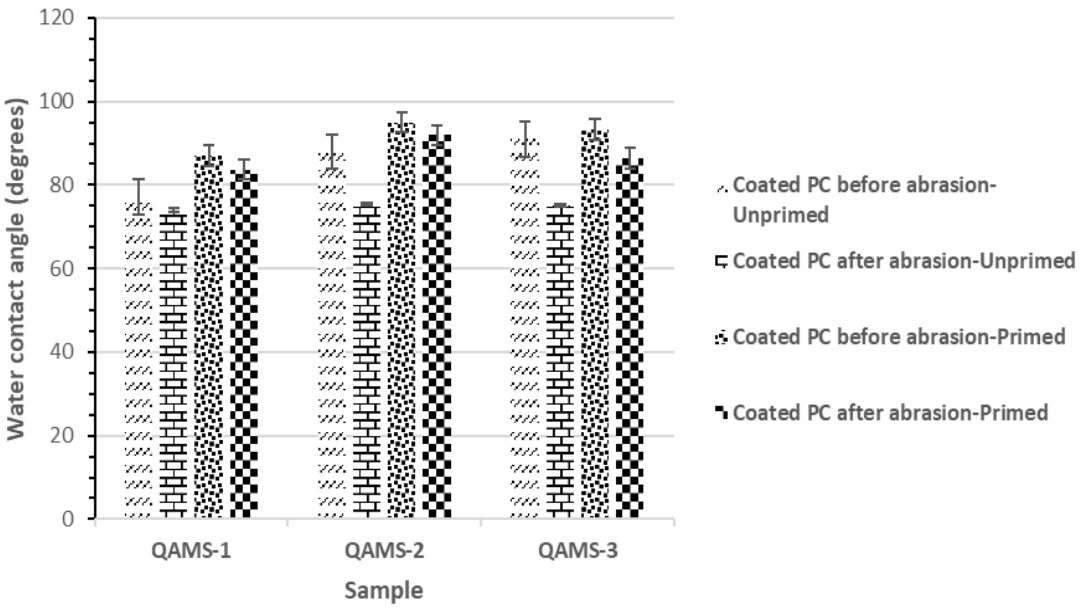

Figure 3. Changes in hydrophobicity of coatings on polycarbonate substrates before and after abrasion.

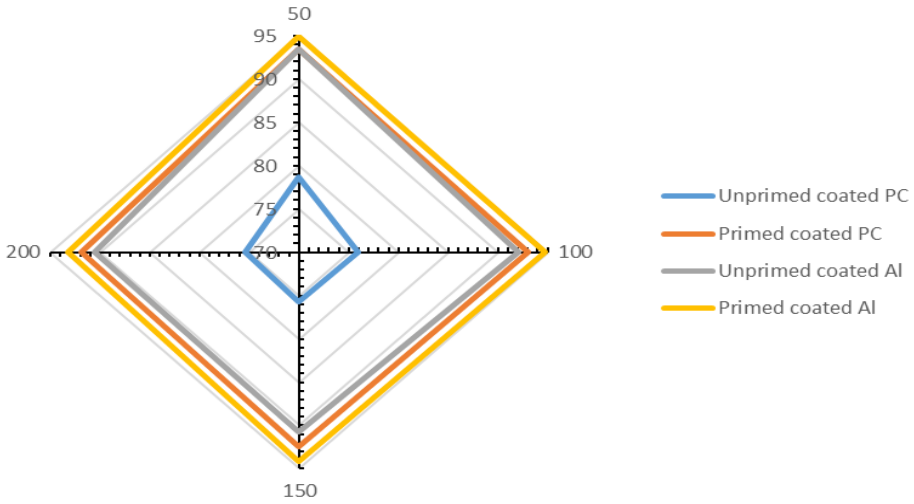

Figure 4. Mean WCA values of coatings on aluminum and polycarbonate substrates after 50, 100, 150 and 200 cycles of abrasion.

3.3. Adhesion

Cross-cut adhesion test was also performed. Classification of results was made according to the following Table 7:

Table 7. Analysis of cross-cut adhesion testing.

Classification result	Description
0	None or 0% area removed
1	Less than 5% area removed
2	5–15% area removed
3	15–35% area removed
4	35–65% area removed
5	Greater than 65% area removed

It was found that all coatings adhered strongly to Al substrates, either primer or unprimed. Adhesion on unprimed PC substrates was sufficient only for thicker coatings. In contrast, priming of the surface resulted in substantially more adherent structures. In this case however, total solids in the topcoat should lie within an optimum range, otherwise thicker structures with limited interconnection occurred. The results of the cross-cut test are summarized in Table 8.

Table 8. Results of cross-cut adhesion testing.

Sample	Classification after adhesion test on coated Al without primer	Classification after adhesion test on coated Al with primer	Classification after adhesion test on coated PC without primer	Classification after adhesion test on coated PC with primer
QAMS-1	0-1	0	3–4	0–1
QAMS-2	0	0	2–3	0
QAMS-3	0-1	0	1–2	1–2

3.4. Hydrolytic stability

Hydrolytic stability of the coatings was evaluated after immersing the coated samples in deionized water at room temperature for 30 d. The samples were weighted and the loss was calculated by the following equation:

$$\text{Weight loss } (\%) = \frac{W_i - W_f}{W_i} \cdot 100\% \quad (1)$$

where W_i and W_f, are the initial (before immersion) and final (after immersion) weight of the samples, respectively.

Results were mostly indicative, since coated samples were thin (~150–250 nm) and therefore variations in weight might contain a significant amount of error. As a rule of thumb however, it was found that the hydrolytic stability of the coatings was, in all cases, acceptable. Compared to unprimed coated polycarbonate samples the weight losses of unprimed coated aluminum samples were higher by more than 20% and these were attributed to partial corrosion of the substrate and subsequent degradation of the coatings. Furthermore, it was also evident that priming aluminum substrates before coating had a prominent effect on the stability of the entire structure, especially when the top coat contained fewer solids. This was a clear demonstration of the well-known barrier properties of the polysilazane primer.

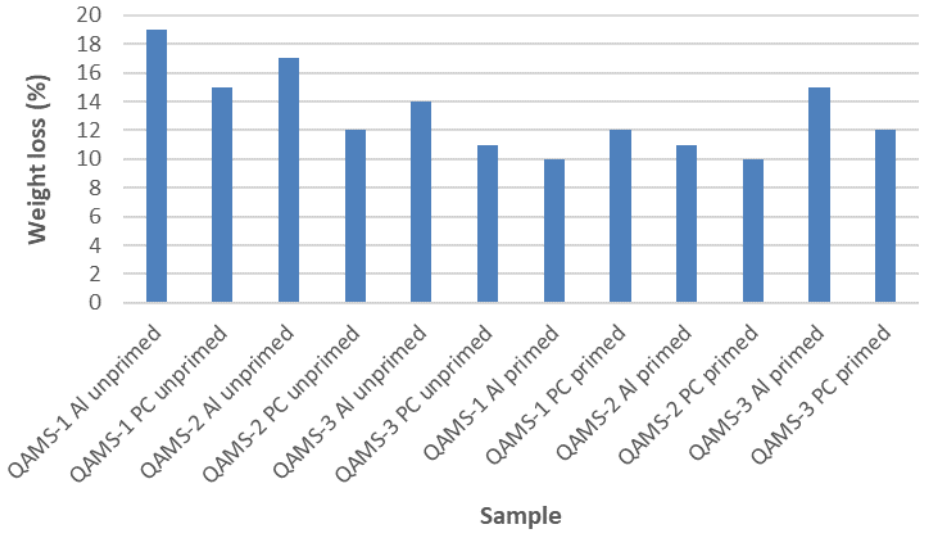

Figure 5. Hydrolytic stability of various compositions of primed and unprimed coatings on Al and PC substrates.

3.5. UV stability

The radiation emission in the UV range, i.e., below 400 nm, is minimum 80% of total emission. Therefore, both primed and unprimed coated specimens were exposed to UV radiation, elevated temperatures and water condensation to reproduce weathering effects, which can appear in reality and in typical outdoor environments. Only coated aluminum specimens were tested, since polycarbonate substrates were prone to UV degradation. The results are presented in Figure 6.

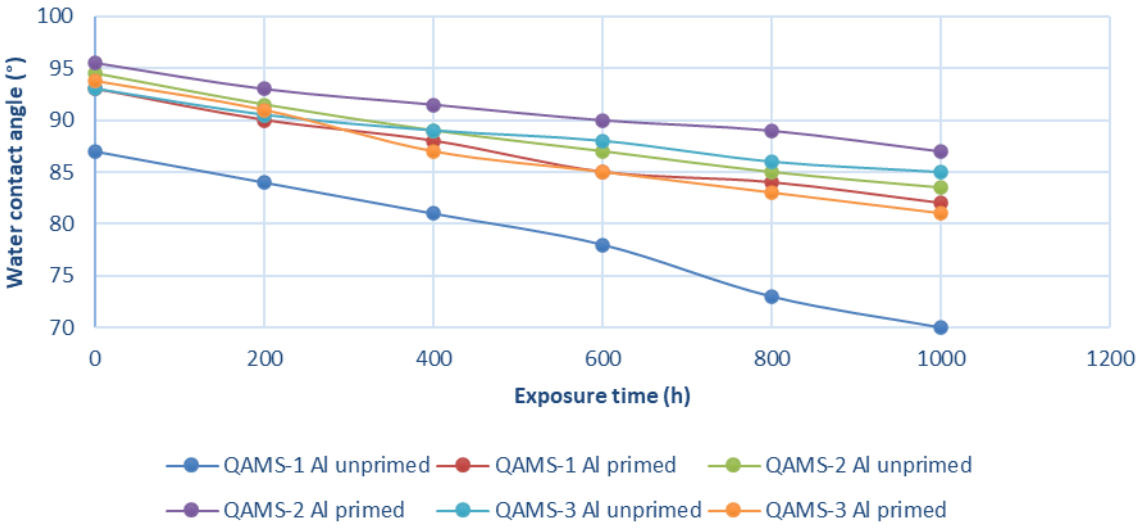

Figure 6. UV stability of various compositions of primed and unprimed coatings on Al substrates.

It was found that hydrophobicity decreased almost linearly with exposure time of UV irradiation. Except from the unprimed Al coating with the lowest solids' weight the WCAs of all

irradiated samples remained well over 80 º, thus implying sufficient UV stability and acceptable functionality even after 1,000 h of exposure. The slope of the curve was quite abrupt in the case of the QAMS-1 unprimed sample, probably because this coating was the thinnest among the ones examined. Both the use of the primer and thickness of the coating seemed to have a positive contribution to the coating stability. With regards especially to the role of the primer, ambient curing of the two adjacent layers led to strong interconnection between them, probably due to the formation of inherently UV-stable Si-N-Si frameworks.

3.6. Chemical resistance

Chemical resistance of both unprimed and primed coatings was evaluated through the reduction in hydrophobicity after immersing coated samples in various reagents for 7 d. The reagents examined were distilled water (cold and hot), ethyl alcohol solution in water (50% v/v), glacial acetic acid solution in water (3% v/v, pH = 3), alkaline aqueous solutions (pH = 9 and pH = 12), acidic aqueous solution (pH = 1), a detergent (Classic Ajax cleaner) and an organic solution (Shellsol D7). Only samples exhibiting the highest WCA values, i.e., QAMS-2 were subjected to this test, since hydrophobicity, and presumably chemical resistance, were the result of enhanced crosslinking. Similar to the abrasion resistance results, it was found that primed coated aluminum substrates had excellent chemical resistance. This was attributed, first, to the chemical resistance of the OPSZ primer itself and to its strong adhesion to the substrate, and secondly, to the strong grafting ability of the topcoat onto the primer. With regards to polycarbonate, it was obvious that the lack of hydroxylated groups inhibited adequate wetting of the substrate and alkoxysilane crosslinking enhancement. Not surprisingly, chemical resistance of unprimed coated samples was found to be rather poor.

Table 9. Chemical resistance of coated substrates immersed into several liquid solutions for 7 d.

Test reagents	Coated primed Al	Coated Al without primer	Coated primed PC	Coated PC without primer
1. Distilled water (cold or hot)	•••	•••	•••	••
2. Ethyl alcohol solution (50% v/v)	•••	•••	••	•
3. Acetic acid solution (3% v/v) (pH = 3)	•••	••	•••	•
4. Alkaline aqueous solution (pH = 9)	•••	•••	•••	••
5. Classic Ajax	•••	•••	••	•
6. Shellsol D7	•••	••	•	/
7. Acidic aqueous solution (pH = 1)	••	•	•	/
8. Alkaline aqueous solution (pH = 12)	••	•	•	/

••• = excellent, •• = very good, • = good, / = not resistant.

In contrast, being a pre-ceramic material, the OPSZ improved both chemical and mechanical resistance of the coating system on PC substrates. Condensation of the two layers proceeded simultaneously, hence, the resulting nanostructure demonstrated advanced chemical stability. In Figure 7, a graphical comparison of the results presented in Table 9 between primed and unprimed coatings on aluminum and polycarbonate substrates is presented.

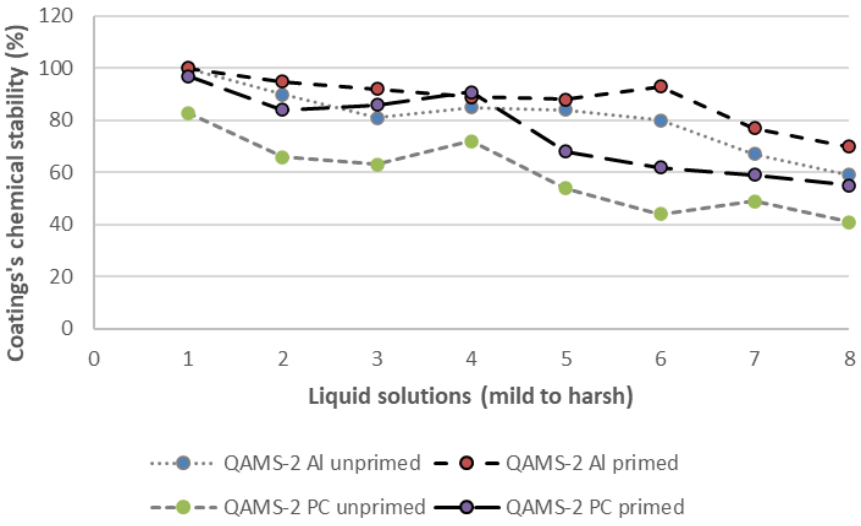

Figure 7. Chemical resistance of primed and unprimed coatings on Al and PC substrates.

3.7. Surface topography by Atomic Force Microscopy

The surface topography and mean roughness of the coatings was evaluated by AFM (Figures 8 and 9). Only the QAMS-2 composition was evaluated. Coatings on unprimed Al substrates presented good uniformity (Figure 8) with however relatively high surface roughness, which in-part was caused by the substrate's inherent topography. The coating's mean surface roughness was significantly reduced after priming of the substrate at the expense however of a slightly degraded uniformity, perhaps due to increased thickness.

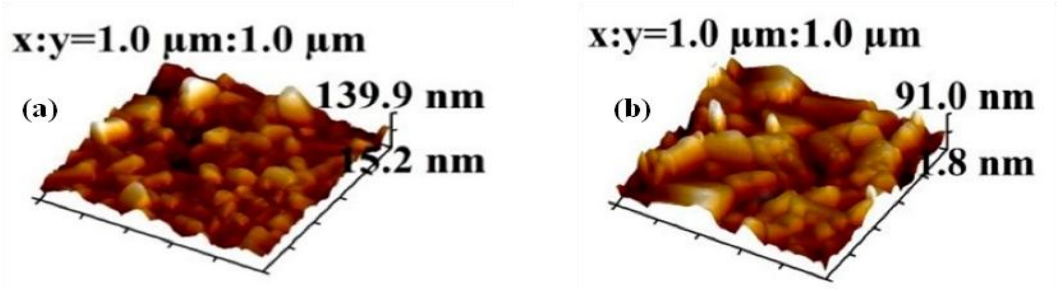

Figure 8. AFM images of coatings on unprimed (a) and primed (b) aluminum substrates.

Concerning PC substrates, it was found that unprimed coatings had limited uniformity with several irregularities (Figure 9). In contrast, although not completely planar, primed coated samples exhibited low surface roughness and good uniformity, without voids or islands.

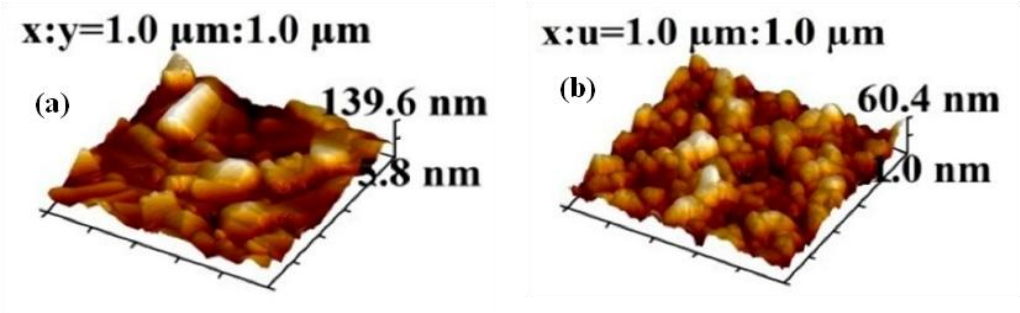

Figure 9. AFM images of coatings on unprimed (a) and primed (b) polycarbonate substrates.

3.8. Microstructure study by Scanning Electron Microscopy

Morphology and microstructural features of coatings were examined by scanning electron microscopy. Similar to AFM analysis, only the QAMS-2 composition was evaluated. Figure 10a–f shows plane and cross-section views of QAMS-2 coatings on aluminum and polycarbonate substrates.

Plane view of the unprimed coating on aluminum (Figure 10a) revealed moderate heterogeneity. After priming (Figure 10c) uniformity was improved. However, minor heterogeneity within the 50–100 nm range was still apparent. Various growth orientations with multiple cross-section curvatures, as well as small indentations were also evident. The cross-section view of the primed-coated sample (Figure 10e) revealed sufficient interconnection of the primer with both the substrate and the top coat, as well as excellent step coverage. The plane views of the coating on polycarbonate revealed a significant improvement in top coat's uniformity after priming (Figure 10b,d). The cross-section view of the primed-coated sample (Figure 10f) confirmed that the cohesion of the primer with the substrate and the top coat was strong. The primer adhered well to the substrate, while the coating had excellent step coverage. No micro/nano-voids, cracks, tearing or detachments were observed. In addition, the air side of the coating appeared rather smooth, which probably enabled highly effective non-stick attributes.

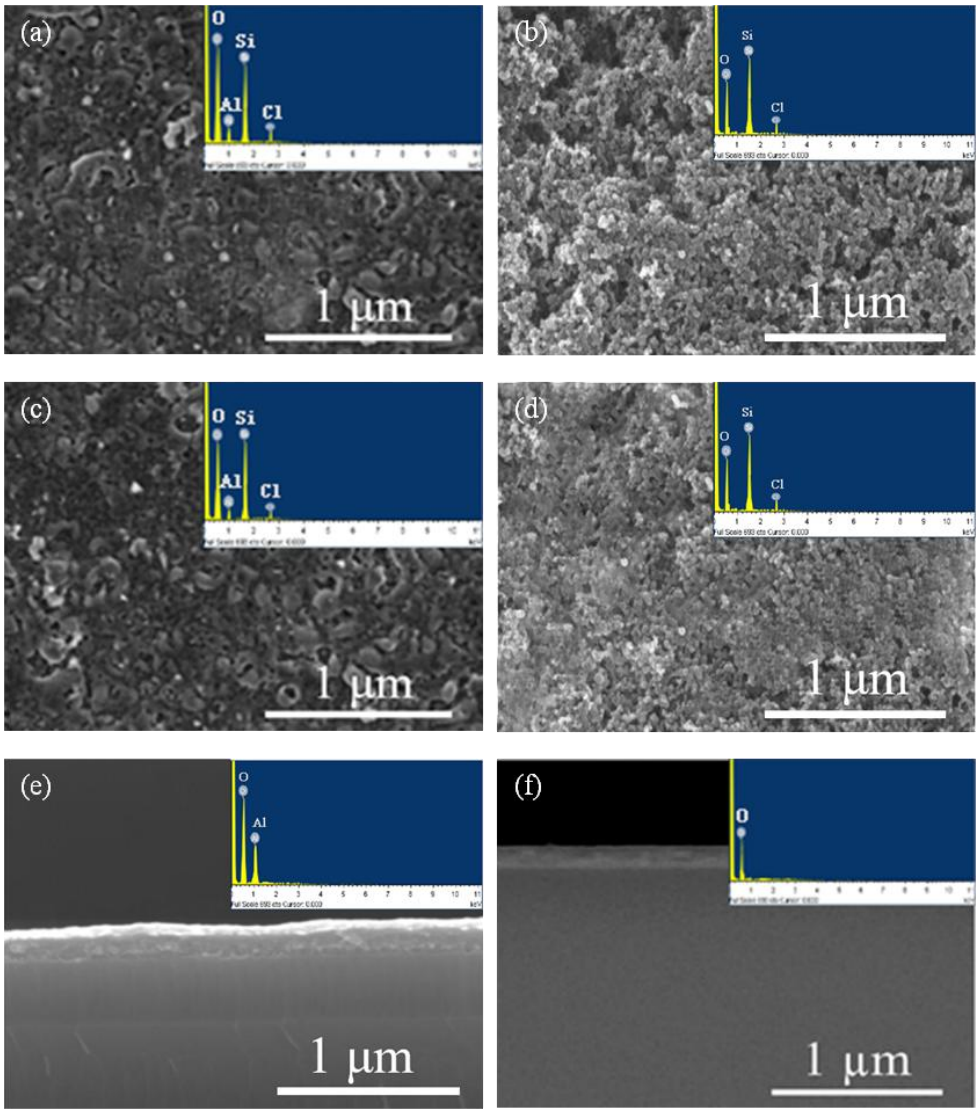

Figure 10. SEM images and EDS analysis of QAMS-2 coating. Plane views on (a) unprimed aluminum, (b) unprimed polycarbonate, (c) primed aluminum and (d) primed polycarbonate. Cross-sections of QAMS-2 coating on (e) aluminum and (f) polycarbonate substrates.

EDS analysis confirmed that the coatings were successfully deposited on both Al and PC substrates. In all samples, the detections of Si and O in relatively high levels indicated the presence of a dense siloxane network. The EDS spectra of unprimed coated Al sample revealed higher concentrations of Al and O, which apparently resulted from the aluminum substrate's native oxide layer. Finally, Cl originated from the top coat's antimicrobial agent.

3.9. Anti-static properties

Anti-static properties of the coatings were indirectly evaluated through the reduction in their transmittivity. Light transmittance of the coated substrates after soiling with dust were compared to the transmittance of unsoiled substrates. The optical transmittance drop of each sample was then

correlated to dust accumulation. Only polycarbonate samples were subjected to testing since coated aluminum substrates were opaque. More specifically, four coated polycarbonate substrates with an initial transmittivity of around 89% were subjected to soiling testing. The first two (samples QAMS-2-Un and QAMS-2-P) referred to QAMS-2 samples with and without the primer, respectively. The other two (Ref-A and Ref-B) referred to two commercial anti-soiling coatings, the first one being hydrophilic, while the other one being hydrophobic. For each sample five cycles of soiling tests were employed. For reasons of simplicity, transmittance losses were considered to be proportional to dust accumulation.

As it can be observed in Figure 11, there was a strong correlation between dust accumulation, transmittance and surface energies of the coatings. The proposed coating of this work exhibited strongwater repellency. The use of the primer (QAMS-2-P sample) promoted further the hydrophobic properties of the coating, although these seemed to be dictated by the antistatic functions of the quaternary ammonium silane molecules, rather than the coatings' ability to repel water. This was clearly evident by comparing QAMS-2-Un sample with Ref-A sample. The latter performed better only in the first soiling cycles where accumulation of dust was limited. Beyond a certain point, the hydrophilic nature of Ref-A sample was unable to provide sufficient self-cleaning attributes against inorganic dust. In contrast, the anti-static performance of QAMS-2-Un was in any soiling cycle decent despite its low initial hydrophobicity (WCA of 88 º). Moreover, it was even close to the performance of Ref-B sample, which exhibited strong initial hydrophobicity with WCAs in the order of 110 º. The above findings highlighted the prominent role that the configuration and polarity of the topcoat had in its anti-static functionality. More specifically, up to a certain concentration of solids in the topcoat, the induced spacing among hydrophobic C-18 chains caused by mutually repelled cationic groups (R_3N^+) forced Si-QUAT molecules to align themselves like vertical nanopillars. The localized polarity of the latter could then attract moisture which prevented dust accumulation. In contrast, beyond a certain concentration ratio of solids it was expected that Si-QUAT molecules would entangle themselves, therefore discrete charge dissipation would probably be diminished.

The mean values of all the above results for both primed and unprimed coatings are summarized in Figure 12.

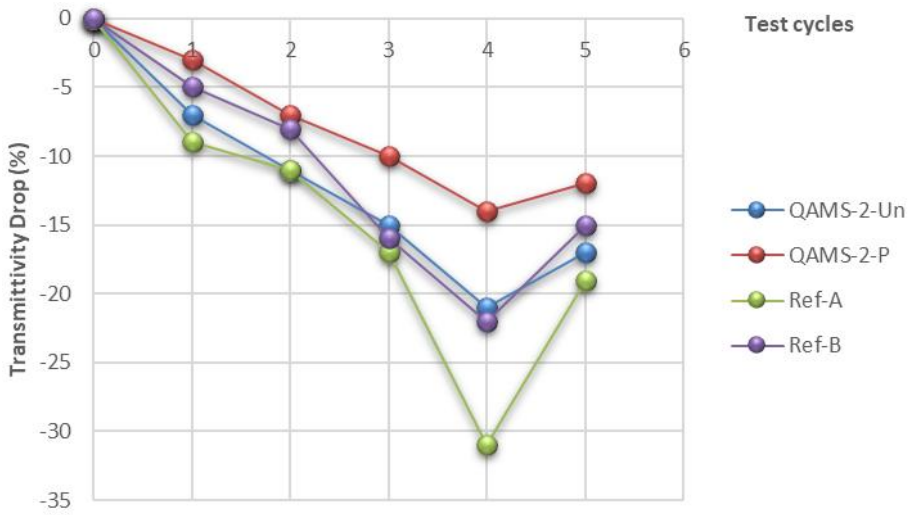

Figure 11. Correlation of coating's anti-soiling properties with its optical transmission drop.

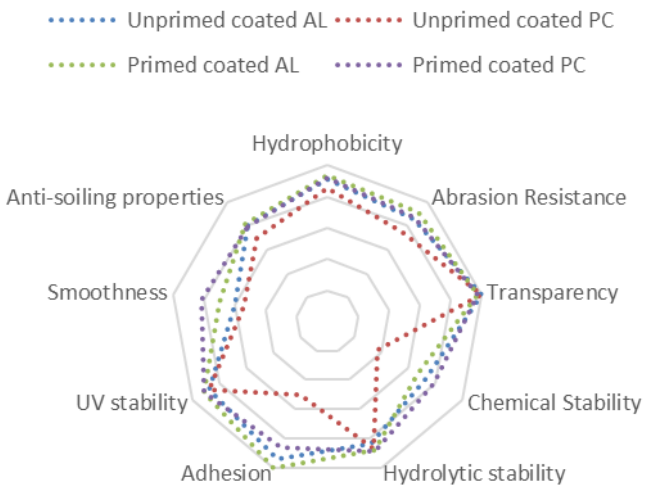

Figure 12. Schematic illustration of the performance of the proposed coating on both primed and unprimed substrates.

4. Further discussion

Silane coupling agents are the primary choice of materials when surface modification is required. In the vast majority of surface treatment applications organofunctional silanes with at least one organic substituent and two or three hydrolysable groups, such as alkoxysilanes, are typically used. The alkoxy groups of the latter are hydrolyzed to form silanol-containing species. Condensation to oligomers follows. The oligomers then hydrogen bond with available –OH groups. In the case of hydroxyl-containing substrates, such as silica, glass and aluminum, durable bonding is strongly promoted. However, even on those surfaces effective surface modification has several limitations, because concentration and type of hydroxyl groups present may vary widely. For example, hydrolytically derived oxides aged in moist air have significant amounts of physically adsorbed water which can interfere with coupling [35].

Hydrogen bonded vicinal silanols react more readily with silane coupling agents, while isolated or free hydroxyls react reluctantly. Poor hydrolytic stability of the oxane bond between the silane and the substrate may be another reason for ineffective surface modification. In the case of iron oxide, nickel and zinc, for example, the resulting bonds are unstable.

In addition, surface modification is maximized when silanes can react with the substrate surface and the latter has an adequate number of accessible sites with appropriate surface energies. In the case of plastics however, this is not the case, therefore complex surface preparation is usually required.

In general, common organofunctional silanes can modify surfaces in order to generate a functional micro-heterogeneous environment or to incorporate the bulk properties of different phases within a single composite structure. They can be either directly deposited on the substrate to promote hydrophobicity or be further modified to yield super-hydrophobicity. When alkoxysilanes are solely added to a formulation as low surface tension components (e.g., fluoroalkoxysilanes), they trigger anti-soiling or self-cleaning attributes, whereas when they are exploited as strengthening materials (e.g. tetraethoxysilane), or as adhesion promoters (e.g. aminopropyltriethoxysilane), they enhance coating robustness [12–25]. However, the afore-mentioned surface modification limitations have an

adverse effect on the coating's adhesive properties, thus keeping its functionality and performance far from optimum levels.

Current practices are unable to mitigate the problem. For example, incorporation of metal or silica nanoparticles into silica inorganic or hybrid organic/inorganic systems usually leads to loosely adhered structures to the substrate, which, in turn, degrades hydrophobicity. Moreover, transparency of the substrate may also be negatively affected [36]. Continuing with polydimethylsiloxanes, they are advantageous due to their flexibility, lubricity and good water-repellency properties [28,37]. However, they exhibit low reactivity towards other functional components (i.e., polysilazanes or polymeric binders), therefore adhesion is adversely affected. Furthermore, although common polymeric binders modified with organofunctional silane coupling agents can create a permanent anti-soiling coating for various substrates, their increased film-thickness may reduce transmittivity and inhibit the application of the resulting coatings on high-end devices, such as electronics or solar panels. Finally, when polysilazanes are the sole component of the coating composition, sufficient hydrophobic, chemical, and mechanical properties are developed [29], at the expense, however of the coating's optical properties, due to increased coating thickness. Reducing the concentration of actives to achieve lower coating thicknesses is not really a viable alternative, since hydrophobity and stability of thin polysilazane-based films are degraded in a non-linear manner.

Considering the above, the development of a two-step coating system, which combines the mechanical durability that polysilazanes provide on a variety of materials with the anti-soiling attributes of a quaternary ammonium silane presents a viable perspective. The concept of depositing the functional layer on top of a primer to enhance the mechanical strength of the overlay structure is not new. In fact, it is a common practice in certain applications, such as thick marine coatings, where the primer acts as a binding material between the substrate and the coating, as well as a protective layer against substrate corrosion. This approach is also effective on plastic substrates [38,39] such as glass reinforced plastics, however it has limited applicability when the coating has to be optically clear. Towards this end, chemical functionalization of acrylic and polycarbonate substrates with thin layers of silane adhesion promoters, such as amino- or epoxy-silanes has been also reported [40]. It has been assumed that surface free radicals promote adhesion due to the formation of weak amide or urethane bonds. The success of this approach is however questionable, since the primary bonding mechanism of silane adhesion promoters with the substrate remains the same with that of common alkoxysilanes.

The proposed coating scheme exploits the mechanical stability of polysilazane monolayers with the anti-soiling and anti-static functions of the silane quaternary compound. The latter adheres strongly to the underlying layer, due to condensation of adjacent silanol groups. This process is further promoted by the strong electrostatic attraction between the cationic groups of the top coat and anionic free radicals of the substate. The resulting structure obtains an improved mechanical stability even on substrates that do not favor surface modification without impairing their aesthetics.

5. Conclusions

- A versatile approach for the development of a two-step anti-soiling coating system comprising a polysilazane primer and a quaternary ammonium silane top-coat is proposed.
- The coating system is transparent and has generic applicability regardless of the type of substrate.

- Sufficient hydrophobicity, UV and hydrolytic stability, marked chemical and abrasion resistance and pronounced anti-static behavior were manifested.
- Smooth coatings with adequate adhesion and excellent step coverage were obtained. No micro/nano-voids, cracks, tearing or detachments were observed.
- The proposed system is suitable for both commercial and industrial applications.
- Development of multilayer structures based on the coating's composition in order to achieve permanent super-hydrophobicity is an additional possibility worth exploring and is currently underway.

Acknowledgments

This research has been co-financed by the European Regional Development Fund of the European Union and Greek national funds through the Operational Program Competitiveness, Entrepreneurship, and Innovation, under the call RESEARCH-CREATE-INNOVATE (project code: T1EDK-04949).

The authors also thank Mrs Panayiota Koutsaftiki for her contribution in developing the schematics of chemical structures.

Conflict of Interest

All authors declare no conflicts of interest in this paper.

References

1. Chundi N, Kesavan G, Ramasamy E, et al. (2021) Ambient condition curable, highly weather stable anti-soiling coating for photovoltaic application. *Sol Energy Mater Sol Cells* 230: 111203. https://doi.org/10.1016/j.solmat.2021.111203
2. Ganesh VA, Raut HK, Nair AS, et al. (2011) A review on self-cleaning coatings. *J Mater Chem* 21: 16304. https://doi.org/10.1039/c1jm12523k
3. Kim D, Kim JG, Kim T, et al. (2021) Long-lasting superhydrophilic and instant hydrophobic micropatterned stainless steel surface by thermally-induced surface layers. *Int J Precis Eng Manuf-Green Technol* 8: 435–444. https://doi.org/10.1007/s40684-020-00207-5
4. Zhang H, Liu H, Chen T, et al. (2021) Fabrication of a fast curing super-hydrophobic FEVE/MMA coating and its property research. *Mater Sci Eng B* 263: 114746. https://doi.org/10.1016/j.mseb.2020.114746
5. Zhou Y, Liu C, Gao J, et al. (2019) A novel hydrophobic coating film of water-borne fluoro-silicon polyacrylate polyurethane with properties governed by surface self-segregation. *Prog Org Coat* 134: 134–144. https://doi.org/10.1016/j.porgcoat.2019.04.078
6. Gao M, Wu X, Gao P, et al. (2019) Properties of hydrophobic carbon-PTFE composite coating with high corrosion resistance by facile preparation on pure Ti. *Trans Nonferrous Met Soc China* 29: 2321–2330. https://doi.org/10.1016/S1003-6326(19)65138-1
7. Xue Y, Wang S, Xue Y, et al. (2020) Robust self-cleaning and marine anticorrosion super-hydrophobic Co-Ni/CeO_2 composite coatings. *Adv Eng Mater* 22: 2000402. https://doi.org/10.1002/adem.202000402

8. Zhang X, Liang J, Liu B, et al. (2014) Preparation of superhydrophobic zinc coating for corrosion protection. *Colloids Surf Physicochem Eng Asp* 454: 113–118. https://doi.org/10.1016/j.colsurfa.2014.04.029
9. Bi, Li, Zhao, et al. (2019) Robust super-hydrophobic coating prepared by electrochemical surface engineering for corrosion protection. *Coatings* 9: 452. https://doi.org/10.3390/coatings9070452
10. Bai M, Kazi H, Zhang X, et al. (2018) Robust hydrophobic surfaces from suspension HVOF thermal sprayed rare-earth oxide ceramics *Coatings. Sci Rep* 8: 6973. https://doi.org/10.1038/s41598-018-25375-y
11. Zhang C, Wu Y, Liu L (2012) Robust hydrophobic Fe-based amorphous coating by thermal spraying. *Appl Phys Lett* 101: 121603. https://doi.org/10.1063/1.4754140
12. Rodič P, Kapun B, Panjan M, et al. (2020) Easy and fast fabrication of self-cleaning and anti-icing perfluoroalkyl silane film on aluminium. *Coatings* 10: 234. https://doi.org/10.3390/coatings10030234
13. Khodaei M, Shadmani S (2019) Superhydrophobicity on aluminum through reactive-etching and TEOS/GPTMS/nano-Al2O3 silane-based nanocomposite coating. *Surf Coat Technol* 374: 1078–1090. https://doi.org/10.1016/j.surfcoat.2019.06.074
14. Liang Z, Zhou Z, Zhao L, et al. (2020) Fabrication of transparent, durable and self-cleaning superhydrophobic coatings for solar cells. *New J Chem* 44: 14481–14489. https://doi.org/10.1039/D0NJ01402H
15. Shang Q, Zhou Y, Xiao G (2014) A simple method for the fabrication of silica-based superhydrophobic surfaces. *J Coat Technol Res* 11: 509–515. https://doi.org/10.1007/s11998-014-9573-z
16. Das S, Kumar S, Samal SK, et al. (2018) A review on superhydrophobic polymer nanocoatings: recent development and applications. *Ind Eng Chem Res* 57: 2727-2745. https://doi.org/10.1021/acs.iecr.7b04887
17. Bouvet-Marchand A, Graillot A, Abel M, et al. (2018) Distribution of fluoroalkylsilanes in hydrophobic hybrid sol-gel coatings obtained by co-condensation. *J Mater Chem* A 6: 24899–24910. https://doi.org/10.1039/C8TA10191D
18. Vidal K, Gómez E, Goitandia AM, et al. (2019) The synthesis of a superhydrophobic and thermal stable silica coating via sol-gel process. Coatings 9: 627. https://doi.org/10.3390/coatings9100627
19. Power AC, Barrett A, Abubakar J, et al. (2016) Versatile self-cleaning coating production through sol-gel chemistry: Versatile self-cleaning coating production. *Adv Eng Mater* 18: 76–82. https://doi.org/10.1002/adem.201500112
20. Purcar V, Rădiţoiu V, Rădiţoiu A, et al. (2020) Preparation and characterization of some sol-gel modified silica coatings deposited on polyvinyl chloride (PVC) substrates. Coatings 11: 11. https://doi.org/10.3390/coatings11010011
21. Özmen E, Durán A, Castro Y (2018) Hydrophobic and oleophobic sol-gel coatings on glass substrates for usage at high temperatures. *Int J Appl Glass Sci* 9: 413–420. https://doi.org/10.1111/ijag.12350
22. Yang Y-Q, Liu L, Hu J-M, et al. (2012) Improved barrier performance of metal alkoxide-modified methyltrimethoxysilane films. *Thin Solid Films* 520: 2052–2059. https://doi.org/10.1016/j.tsf.2011.10.041

23. Liu S, Liu X, Latthe SS, et al. (2015) Self-cleaning transparent superhydrophobic coatings through simple sol-gel processing of fluoroalkylsilane. *Appl Surf Sci* 351: 897–903. https://doi.org/10.1016/j.apsusc.2015.06.016
24. Pratiwi N, Zulhadjri, Arief S, et al. (2020) Self-cleaning material based on superhydrophobic coatings through an environmentally friendly sol-gel method. *J Sol-Gel Sci Technol* 96: 669-678. https://doi.org/10.1007/s10971-020-05389-7
25. Akustia Widati A, Nuryono N, Kartini I, et al. (2019) Water-repellent glass coated with SiO_2-TiO_2-metyhltrimethoxysilane through sol-gel coating. *AIMS Mater Sci* 6: 10–24. https://doi.org/10.3934/matersci.2019.1.10
26. Ghiotti A, Bertolini R, Pezzato L, et al. (2021) Surface texturing to enhance sol-gel coating performances for biomedical applications. *CIRP Ann* 70: 459–462. https://doi.org/10.1016/j.cirp.2021.04.040
27. Bertolini R, Bruschi S, Ghiotti A, et al. (2019) Ultrasonic vibration turning to increase the deposition efficiency of a silica-based sol-gel coating. Procedia Manuf 34: 101–109. https://doi.org/10.1016/j.promfg.2019.06.126
28. Syafiq A, Vengadaesvaran B, Rahim NAbd, et al. (2019) Transparent self-cleaning coating of modified polydimethylsiloxane (PDMS) for real outdoor application. *Prog Org Coat* 131: 232–239. https://doi.org/10.1016/j.porgcoat.2019.02.020
29. Chen Z, Li G, Wang L, et al. (2018) A strategy for constructing superhydrophobic multilayer coatings with self-cleaning properties and mechanical durability based on the anchoring effect of organopolysilazane. *Mater Des* 141: 37–47. https://doi.org/10.1016/j.matdes.2017.12.034
30. Sutar RS, Gaikwad SS, Latthe SS, et al. (2020) Superhydrophobic nanocomposite coatings of hydrophobic silica NPs and poly(methyl methacrylate) with notable self-cleaning ability. *Macromol Symp* 393: 2000116. https://doi.org/10.1002/masy.202000116
31. Suriano R, Ciapponi R, Griffini G, et al. (2017) Fluorinated zirconia-based sol-gel hybrid coatings on polycarbonate with high durability and improved scratch resistance. *Surf Coat Technol* 311: 80–89. https://doi.org/10.1016/j.surfcoat.2016.12.095
32. Zhang LB, Zhang HX, Liu ZJ, et al. (2023) Nano-silica anti-icing coatings for protecting wind-power turbine fan blades. *J Colloid Interface Sci* 630: 1–10. https://doi.org/10.1016/j.jcis.2022.09.154
33. Zhan Y, Grottenmüller R, Li W, et al. (2021) Evaluation of mechanical properties and hydrophobicity of room-temperature, moisture-curable polysilazane coatings. *J Appl Polym Sci* 138: 50469. https://doi.org/10.1002/app.50469
34. Rossi S, Deflorian F, Fedel M (2019) Polysilazane-based coatings: corrosion protection and anti-graffiti properties. *Surf Eng* 35: 343–350. https://doi.org/10.1080/02670844.2018.1465748
35. Arkles B, Silane coupling agents: Connecting across boundaries, Gelest, Inc., 2014. Available from: https://www.gelest.com/wp-content/uploads/Silane_Coupling_Agents.pdf.
36. Ogoshi T, Chujo Y (2005) Organic-inorganic polymer hybrids prepared by the sol-gel method. *Compos Interfaces* 11: 539–566. https://doi.org/10.1163/1568554053148735
37. Gong X, He S (2020) Highly durable superhydrophobic polydimethylsiloxane/silica nanocomposite surfaces with good self-cleaning ability. *ACS Omega* 5: 4100–4108. https://doi.org/10.1021/acsomega.9b03775

38. Chen Z, Liu X, Wang Y, et al. (2015) Highly transparent, stable, and superhydrophobic coatings based on gradient structure design and fast regeneration from physical damage. *Appl Surf Sci* 359: 826–833. https://doi.org/10.1016/j.apsusc.2015.10.150
39. Wu X, Chen Z (2018) A mechanically robust transparent coating for anti-icing and self-cleaning applications. *J Mater Chem A* 6: 16043–16052. https://doi.org/10.1039/C8TA05692G
40. Lee JW, Heo JH, Lee B, et al. (2019) Enhancement in the adhesion properties of polycarbonate surfaces through chemical functionalization with organosilicon coupling agents. *J Mater Sci Mater Electron* 30: 17773–17779. https://doi.org/10.1007/s10854-019-02128-9

AIMS Press